Ann. Geophys., 24, 2877–2889, 2006
www.ann-geophys.net/24/2877/2006/

Annales Geophysicae

Vertical propagation characteristics and seasonal variability of tidal wind oscillations in the MLT region over Trivandrum (8.5° N, 77° E): first results from SKiYMET Meteor Radar

V. Deepa, G. Ramkumar, M. Antonita, K. K. Kumar, and M. N. Sasi

Space Physics Laboratory, Vikram Sarabhai Space Centre, Trivandrum 695022, India

Received: 13 January 2006 – Revised: 20 September 2006 – Accepted: 19 October 2006 – Published: 21 November 2006

Abstract. Tidal activity in the Mesospheric Lower Thermosphere (MLT) region over Trivandrum (8.5° N, 77° E) is investigated using the observations from newly installed SKiYMET Meteor Radar. The seasonal variability and vertical propagation characteristics of atmospheric tides in the MLT region are addressed in the present communication. The observations revealed that the diurnal tide is more prominent than the semi/terdiurnal components over this latitude. It is also observed that the amplitudes of meridional components are stronger than that of zonal ones. The amplitude and phase structure shows the vertical propagation of diurnal tides with vertical wavelength of ∼25 km. However, the vertical wavelength of the semidiurnal tide showed considerable variations. The vertical propagation characteristics of the terdiurnal tide showed some indications of their generating mechanisms. The observed features of tidal components are compared with Global Scale Wave Model (GSWM02) values and they showed a similar amplitude and phase structure for diurnal tides. Month-to-month variations in the tidal amplitudes have shown significant seasonal variation. The observed seasonal variation is discussed in light of the variation in tidal forcing and dissipation.

Keywords. Meteorology and atmospheric dynamics (Middle atmosphere dynamics; Thermospheric dynamics; Waves and tides)

1 Introduction

Atmospheric tides are the strongest perturbations that play a decisive role in controlling the dynamics of the MLT region. By now, it is well established that atmospheric tides are global oscillations with a period of a solar day and its subharmonics. It is also known that they are excited by solar heating of water vapor in the troposphere and ozone in the stratosphere. By realizing the importance of tidal activity, extensive wind observations in the MLT region have been carried out across the globe to explore its structure and dynamics (Tetenbaum et al., 1986; Avery et al., 1989; Manson et al., 1988; Portnyagin et al., 1992; Fraser et al., 1995; Tsuda et al., 1999; Zhang et al., 2004). Extensive studies have been carried out on tidal oscillations in the middle and high latitudes, whereas studies from the low-latitude MLT region are very limited (Reddi et al., 1993; Reddi and Ramkumar, 1997; Chang and Avery, 1997; Gurubaran and Rajaram, 1999). Most of these studies showed that the migrating tides are prominent components in the MLT region and there is considerable latitudinal variation in the tidal structure. The high-latitude observations showed that the semidiurnal component is more prominent than the diurnal component, whereas tropical latitude observations revealed that the diurnal component is stronger (Pancheva et al., 2002; Manson et al., 1999, 2002a). To date, various platforms have been used to study the MLT region winds and among these platforms, MF and meteor radar observations significantly contributed to our present understanding of tidal structure and its variability. However, these observations were unable to provide a global picture of tidal activity in the MLT region. In an attempt to divulge the global aspects of tides, Planetary Scale Mesopause Observing System (PSMOS) campaign has been carried out (Pancheva et al., 2002). Even though these observations have revealed a great deal about various tidal modes in the MLT region, the deployment of ground-based instruments is limited by the geography, such as oceanic regions. There were 22 radars included in the campaign, but the network was not uniformly distributed, and representation of tropical stations was rather sparse. However, by the introduction of satellite observations of mesosphere and lower thermosphere neutral winds, a global coverage on the atmospheric tides in the MLT region was obtained. Measurements using the HRDI and WINDII onboard UARS have

Correspondence to: G. Ramkumar
(geetha_ramkumar@vssc.gov.in)

Published by Copernicus GmbH on behalf of the European Geosciences Union.

Table 1. System specification of SKiYMET Meteor Wind Radar at Trivandrum (8° N, 77° E).

System specifications	
Peak power	40 kW
Frequency	35.25 MHz
PRF	2144 Hz
Pulse width	13.3 μm
TX antenna	Four circular polarized 3-element Yagi (crossed elements) at the corners of a square
RX antenna	Five circular polarized 2-element Yagi (crossed elements) spaced to form an interferometer

provided a better understanding of the global picture of tides (Morton et al., 1993; Burrage et al., 1995a, b; McLandress et al., 1996; Manson et al., 1999, 2002a, b; Zhang et al., 2004). The HRDI gives night-time wind data at 95 km only (Talaat and Lieberman, 1999). But WINDII provides daytime green-line observations four times per week and night measurements twice per week. In practice, several months of data are required to provide adequate local time coverage (Mc Landress et al., 1996; Hagan et al., 1997). Zonal averaging is also done to extract tidal information (Mc Landaress et al., 1996). Thus satellite measurements provide only an average picture of tidal oscillations.

A significant modeling effort has been made to understand the mean global variation of tidal components (Forbes and Vial, 1989; Hagan, 1996; Hagan et al., 1999; Hagan and Roble, 2001; Hagan and Forbes, 2002, 2003). Hagan et al. (1995) developed the two-dimensional, linearized, steady-state numerical tidal model, known as the Global Scale Wave Model (GSWM). Some of the above-discussed studies made an effort to compare the observed tidal features with the model values. Chang and Avery (1997) made a detailed study on tidal activity and compared their observations with GSWM. They attributed the discrepancy in the comparisons to the effects of nonmigrating tides. Most of the other comparison studies reported impressive agreement between the models and observations of tidal phases. But there are disturbing differences in tidal amplitudes, especially that the seasonal and latitudinal variability of tidal amplitudes have shown considerable disagreement with the model values.

It is clear from the above discussion that the large degree of tidal variability and the limited available observations, even with the UARS coverage, makes the establishment of a complete tidal climatology very difficult to achieve. To overcome these difficulties a greater number of uniformly distributed networks of ground station observations across the globe are needed. Realizing the importance of these studies, a state-of-the-art meteor wind radar has been installed at Trivandrum (8.5° N, 77° E) to continue the efforts of exploring the MLT region dynamics.

In the present study, the month-to-month variation of vertical characteristics of atmospheric tides in the MLT region, using the all-sky interferometric meteor (SKiYMET) radar at the low-latitude station Trivandrum (8.5° N), is presented. The horizontal wind observations from the radar system are used for the tidal analysis and to study its seasonal variability. These are the initial results from the radar observations, which are compared with GSWM02 (Hagan and Forbes, 2002, 2003) model values. This study serves to assess the present understanding of the tidal characteristics in the low-latitude MLT region and to compare the GSWM02 values with the observations over this latitude.

In Sect. 2 the data analysis and system details are described. The results are discussed in Sect. 3. A summary and conclusions are given in Sect. 4.

2 Data and method of analysis

The wind observations from the SKiYMET Meteor Wind Radar, which became operational from June 2004, are used for the present study. This radar system operates at 35.25 MHz, with a peak power of 40 kW, and is the most powerful radar of its kind. The system specifications are given in Table 1. A special transmitting scheme has been worked out to avoid the echoes from the Equatorial Electro Jet (EEJ). Four transmitting antennas at the corners of a square are employed for this purpose. One pair of antennas transmits out of phase with the other, such that a null field will be formed at the overlapping region of the beams, thus avoiding echoes from the EEJ region. Five separate receivers are used for data acquisition, one for each antenna. This allows interferometry to be performed in order to determine the position of the meteor trail in the sky, without ambiguities in the angle of arrival. The radar system utilizes state-of-the-art software and computing techniques to acquire, detect, analyze and display meteor entrance events. By observing how the meteor trail drifts with time, deductions can be made about the speed and direction of the atmospheric wind at the altitude at which the meteor was observed. The instrument detects a sufficient number of meteor echoes throughout the day, to derive a comprehensive picture of the wind field. Analysis of the decay time of the meteor trail allows the determination of absolute measurements of mesospheric temperatures. Radial velocity can be measured with an accuracy of 5% or better and temperature with 10 K or better.

The horizontal wind is obtained by measuring the radial velocity of every meteor detected and then combining these measurements in an all-sky manner. Radial velocities are determined by using both auto- and cross-correlation functions associated with meteor detections, and using the rate of change of phase near zero lag to determine the radial velocity (Hocking et al., 2001). The horizontal wind data at every hour with an altitude resolution of $\sim$3 km in the 80–100 km altitude region is used for the present study. All zonal

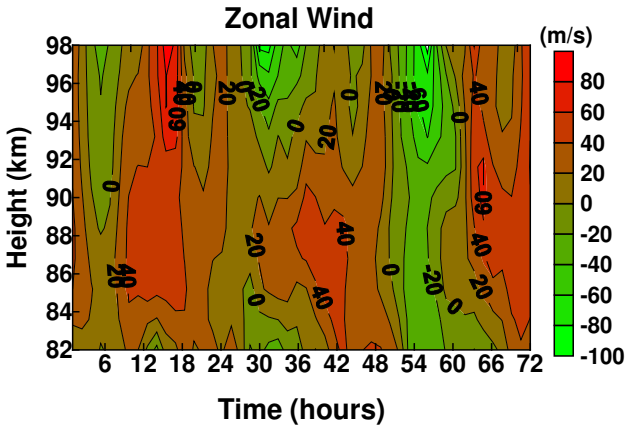

Fig. 1. Time-height contour of the zonal wind observed during three consecutive days (72 h). Red contours represent the westerly winds and green the easterly winds.

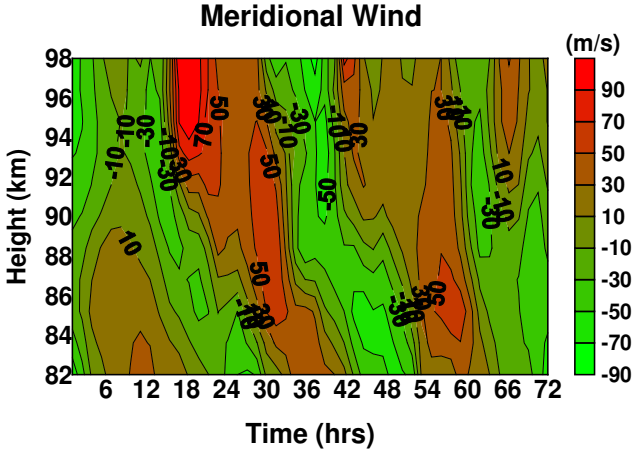

Fig. 2. Time-height contour of the meridional wind observed during three consecutive days (72 h). Red contours represent the southerly winds and green the northerly winds.

and meridional velocities in a month are averaged in hourly bins, at each altitude, to form a 30-day-based composite diurnal cycle. This composite cycle provides a better representation of the tidal structure for a particular month, than a single day or 10-day diurnal cycle. The composite diurnal cycles are obtained for every month from June 2004 to May 2005 and subjected to Fourier analysis, to obtain the altitude structure of amplitudes and phases of different tidal components. The following section describes the results obtained from the present analysis. From the vertical profiles of amplitude and phase, vertical propagation characteristics of tidal oscillations can be studied.

3 Results and discussion

Figures 1 and 2 show the time height variation of zonal and meridional winds for three consecutive days, i.e. from 1 to 3 July 2004. The red contours represent the westerly and southerly winds and green that of the easterly and northerly. These figures clearly reveal the presence of a diurnal tide in the present observations. The wind contours tilt downward with increasing time, indicating the upward propagation of the wave energy, which is more clear in the case of meridional winds.

3.1 Diurnal tides

Figure 3 represents the altitude profiles of amplitude and phase of zonal diurnal tide for all the months, along with the GSWM02 model values (Hagan and Forbes, 2002, 2003). The GSWM02 is a 2-D model that employs observed distributions of background winds (from HRDI data), temperatures (MSISE 90 model), ozone (HALOE) and water vapor. It includes dynamical processes, such as eddy diffusion and gravity wave drag. In this model nonmigrating components of tidal oscillations are also taken into account. The height profiles of amplitude show an increasing trend with height during all the months except for June. The observed amplitudes are in the range of 10 to $\sim$60 ms^{-1}. The standard error in the amplitude measurement is in the range 0.1–0.2 ms^{-1}, whereas in phase it is $\sim$0.1 h. Relatively low amplitude values are observed during June, July, April and May, whereas amplitudes reaching up to 50–60 ms^{-1} are observed during equinoxes, i.e. during September, October and March. These amplitude values are consistent with that observed by Mc Landress et al. (1996) with WINDII data. The observed amplitudes are larger than that observed by Gurubaran and Rajaram (1999) over a nearby location Thirunelveli (8.7° N, 77.8° E). It can be noted that the amplitude of zonal wind remains more or less constant with height during June and July. During April and May the growth of amplitude with height is also very weak. Studies over Christmas Island also showed that during April, May and June the growth of the zonal wind amplitude with height is very weak (Chang and Avery, 1997). The phase profiles show downward propagation with time, indicating upward wave energy flux. The phase values are consistent with model values except for June, July and April. These phase profiles are used to estimate the vertical wavelengths, which are found to be $\sim$25 km. This wavelength is consistent with that of the (1,1) mode of the migrating diurnal tidal component (Forbes and Groves, 1987).

Figure 4 shows the altitude profiles of amplitude and phase for meridional diurnal tides for different months. The amplitude of meridional diurnal tides is greater than that of zonal component. The GSWM02 model values also show that over this latitude the diurnal tidal amplitudes of the meridional wind are larger than that of zonal winds. The observations over other low latitude stations, such as Tirnelveli (8.7° N) (Gurubaran and Rajaram, 1999) and Christmas Island (2° N), (Chang and Avery, 1997; Manson et al., 1999; Tsuda et al.,

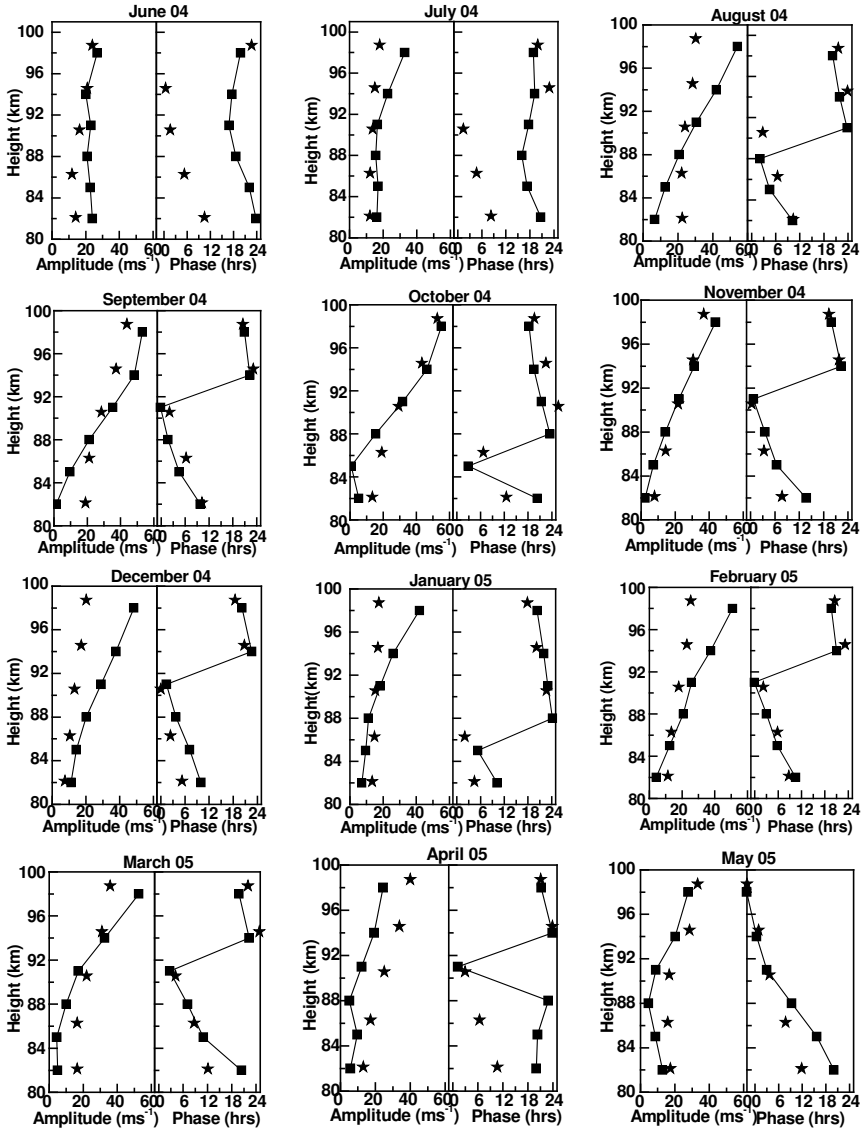

Fig. 3. Height profile of amplitude and phase of zonal diurnal tides from June 2004 to May 2005. Squares represent the observed values and stars represent the GSWM02 model values.

1999), also reported that the amplitude of the meridional diurnal tide is greater than that of zonal diurnal component. The amplitude of meridional winds increases up to 90 km and then decreases during June, April and May. During July the meridional wind amplitude decreases slightly with height. Similar observations are seen over Christmas Island which shows that the meridional wind amplitudes increase to $\sim$50 ms^{-1}, up to the altitude of 90 km and then decreases during April, May, June and July (Chang and Avery, 1997; Mansion et al., 1999). But the observations over Thirunelveli (Gurubaran and Rajaram, 1999) show that the diurnal tidal amplitudes decrease up to 90 km and then increases. The amplitude and phase values are consistent with model values, except for the phase values during June, July, December and January; the observed and model values of phase during these months differ by $\sim$6 h. The vertical wavelength of the meridional diurnal component is also $\sim$25 km, indicating that the observed diurnal tidal component is that of a (1,1) mode.

The vertical wavelength of the diurnal component calculated by Chang and Avery is in the range of 50–100 km, in contrast to the present observation of $\sim$25 km. The vertical wavelength of diurnal tides obtained by Gurubaran and Rajaram (1999) over Thirunelveli is in the range of 40–50 km. Earlier observations at tropical stations, such as at Arecibo, Puerto Rico (18° N), using incoherent scatter radar

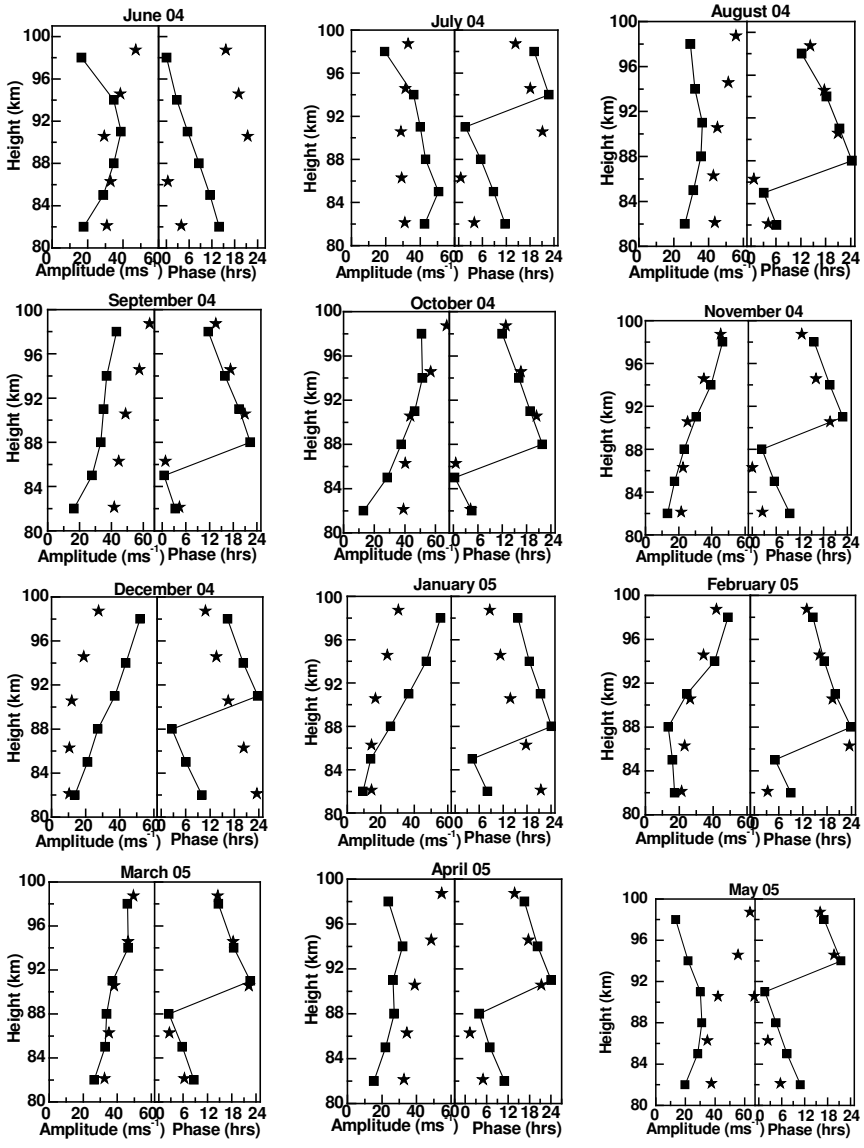

Fig. 4. Same as Fig. 3, but for meridional diurnal tides.

(Mathews, 1976; Harper, 1981; Zhang et al., 2004), and at Punta Borinquen, Puerto Rico (18° N) (Bernard et al., 1981), showed the dominance of diurnal tides with amplitudes ranging from 20 ms^{-1} to 35 ms^{-1} and vertical wavelengths from 25 to 30 km in the 80–100 km height region. Their observations showed that the amplitude of the meridional component is stronger than that of the zonal diurnal tide. Using mesosphere-stratosphere-troposphere radar at Jicamarca, Peru (12° S) Countryman and Dolas (1982) observed strong 24-, 12- and 8-h oscillations in the upper atmosphere, and the vertical wavelength of the 24-h component was observed to be ∼26 km, consistent with the present observations.

During all twelve months the meridional component leads the zonal wind, except at one or two heights in July and December. Phase shifts (PS) between zonal and meridional diurnal tidal components varies with height and with month. During June and July the PS varies from ∼9 h to ∼15 h in the 80–100 km height range. The PS is ∼3 h during August, November, January and February. During September, October, and December, the PS is ∼6 h, which indicates that during these months the zonal and meridional components are in quadrature polarization. From March to May the PS is ∼9 h up to 88 km and above that decreases to ∼3.5 h. The larger amplitude and varying phase shifts between zonal and meridional components indicate the presence of superposed modes. Both zonal and meridional diurnal components during vernal equinox and summer have a significant phase difference of 180° with that observed during autumnal equinox and winter.

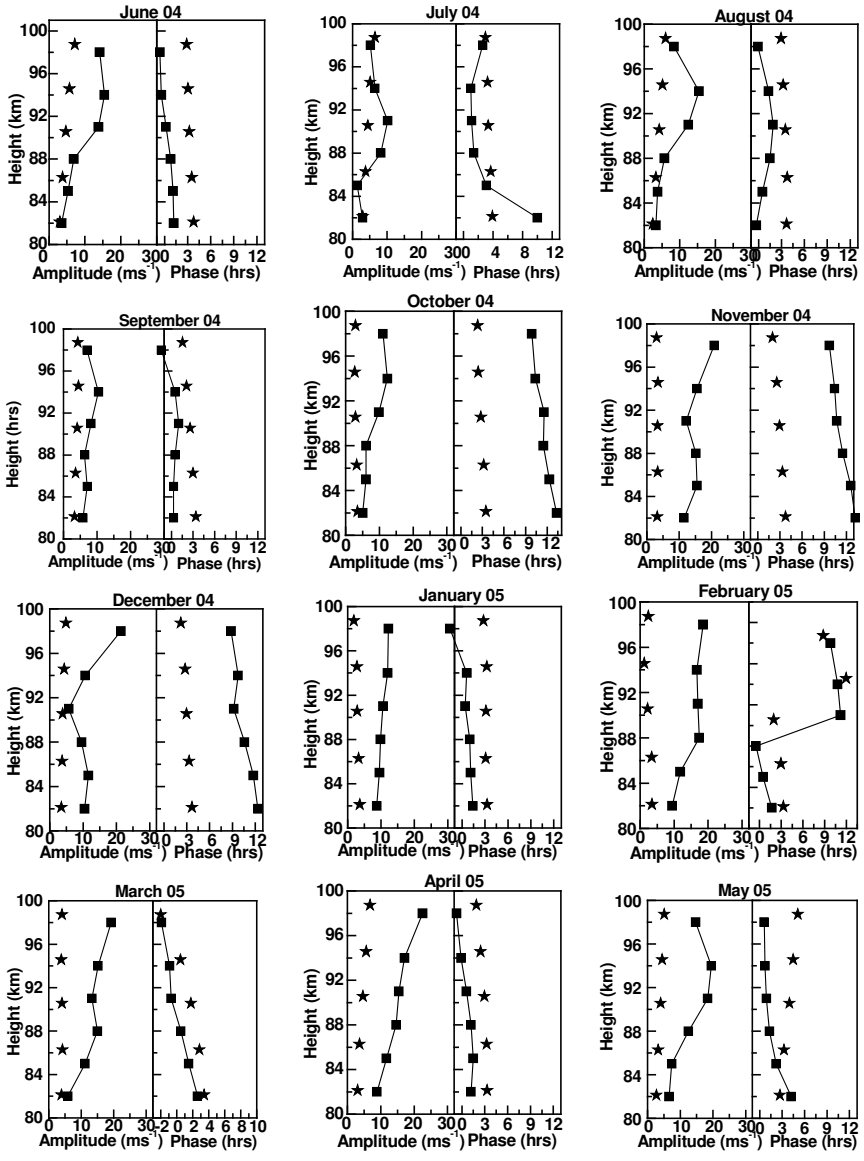

Fig. 5. Same as Fig. 3, but for zonal semidiurnal tides.

3.2 Semidiurnal tides

Figures 5 and 6 show the amplitude and phase profiles of zonal and meridional semidiurnal tides for each month during the present observational period. The amplitude increases with height for both the components, as expected during all the months except for July, August and May, in the case of the zonal component, where the amplitude values increase up to 90 km and then decreases. During September and January the amplitude values remain constant with height. The rate of increase of amplitude with height varies from month to month. The growth of the zonal wind amplitude is larger during November, December, February, March and April (i.e. from 10 ms^{-1} at 82 km to 20 ms^{-1} at 98 km). During other months the amplitude values increase from $\sim$5 ms^{-1} at 82 km to $\sim$10 ms^{-1} at 98 km. The amplitude of the meridional component is greater than that of the zonal component as observed in diurnal tidal amplitudes. The amplitude of the meridional wind increases with height for all the months. From July to October the rate of increase of amplitude with height is larger and reaches a maximum value of 30 ms^{-1} at 98 km. The observed amplitude values are greater than that of the model values. These amplitude values are larger than that observed over Christmas Island (2° N) by Mansion et al. (2002b). Observations at Christmas Island showed that monthly mean semidiurnal meridional amplitudes are in the range of 10–15 ms^{-1} (Burrage et al., 1995b). The amplitude values of semidiurnal tides observed over

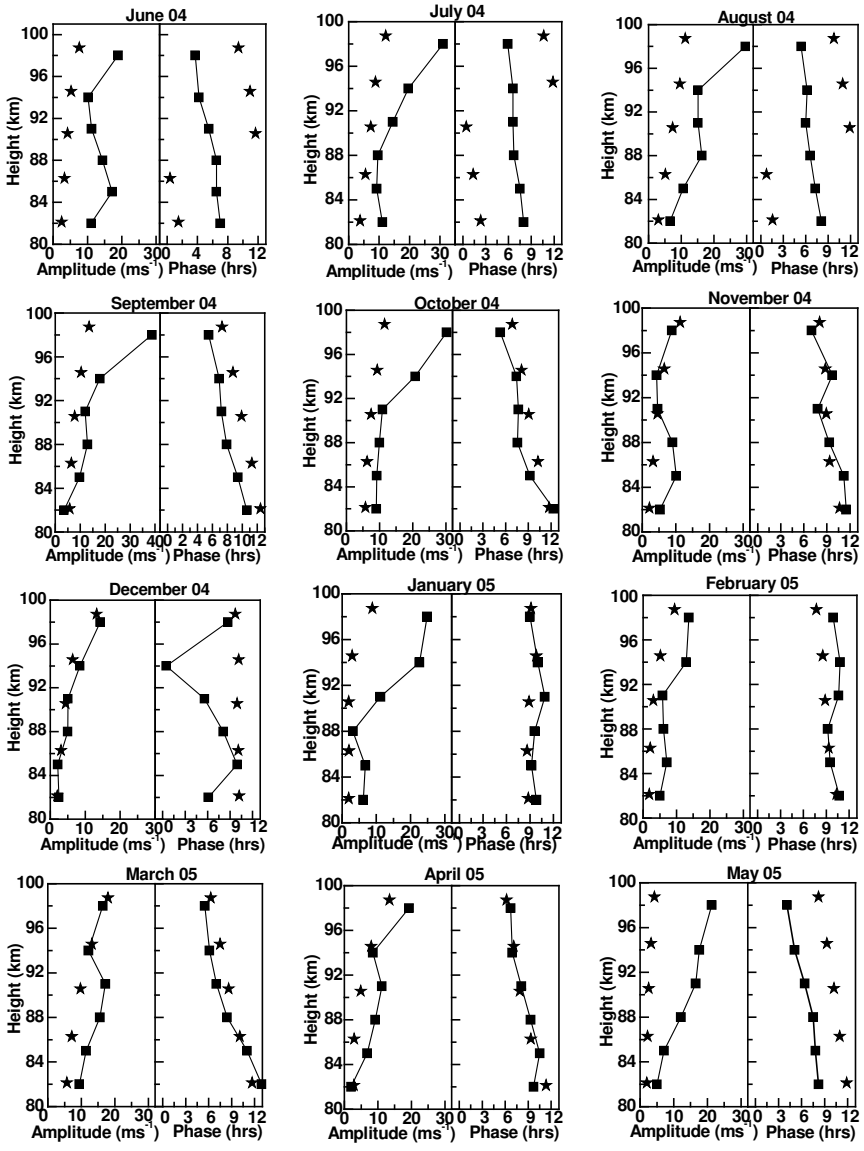

Fig. 6. Same as Fig. 3, but for meridional semidiurnal tides.

Arecibo (18° N), using incoherent scatter radar, is $\sim$15 ms^{-1} (Zhang et al., 2004). The semidiurnal tidal amplitude observed using HRDI wind data at the latitude of $\sim$20° N is $\sim$25 ms^{-1} during April and May and is 20–25 ms^{-1} at the equator during June to August (Burrage et al., 1995b). Thus, the present observations show large, semidiurnal amplitudes in meridional winds as compared to other geographical locations.

It is seen from Figs. 5 and 6 that the phase decreases with height consistently for both zonal and meridional components. The phase structure is similar to that of GSWM02. The observed and model phase values differs by $\sim$3 h during October, November and December for zonal winds. For other months, observed and model phase values are in good agreement. In the case of meridional winds the observed and model values of phase differ by $\sim$4 h during June, July and August. The vertical wavelength calculated from the phase structure shows variation from month to month. The vertical wavelength of the zonal wind is calculated to be $\sim$100 km from June to September. From October to May the vertical wavelength is $\sim$64 km. For the meridional wind the vertical wavelength is $\sim$100 km during January and February. During October to May it is found to be $\sim$64 km. During other months still shorter vertical wavelengths, of the order of 40–50 km, are estimated. The larger vertical wavelengths ($>$100 km) correspond to the vertical wavelength of the (2,2) symmetrical mode (Forbes, 1982). The higher order semidiurnal components, such as (2,4), (2,5) or (2,7), have much

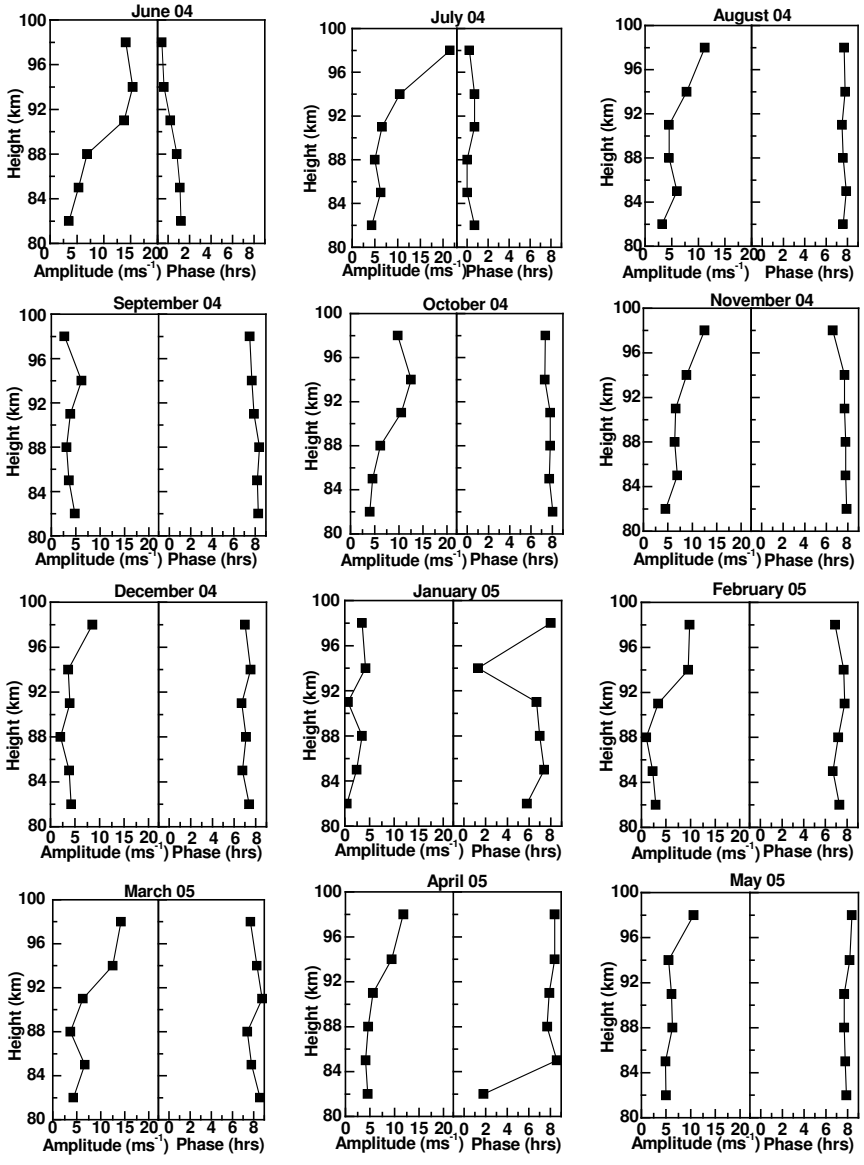

Fig. 7. Same as Fig. 3, but for zonal terdiurnal tides.

shorter vertical wavelength values. The present observations show that the (2,2) mode with wavelength ∼100 km is generally stronger in the zonal wind compared to other modes. Higher order modes show strong signatures in the meridional wind during some months. Forbes (1982) reported that the (2,2) mode grows exponentially up to about 70 km and at higher altitudes its amplitude decreases due to dissipation. Above this altitude, higher order modes (2,4), (2,5) and (2,7) become more prominent. Present observations also show the similar signature and are thus consistent with the earlier studies.

3.3 Terdiurnal tides

Figures 7 and 8 depict the vertical structure of the amplitude and phase of the terdiurnal tide for zonal and meridional components, respectively. The amplitude of the zonal terdiurnal tide increases with height for all the 12 months. The values increase from 5 ms^{-1} to 10 ms^{-1} for both zonal and meridional winds. The maximum zonal wind amplitude observed is 22 ms^{-1} during July. The amplitude of meridional wind increases with height except for July and October. The amplitude of both the zonal and meridional winds increases up to 95 km and then decreases during the month of October. Terdiurnal tides of amplitude 10 ms^{-1} in the zonal component and 5 ms^{-1} in the meridional component were reported

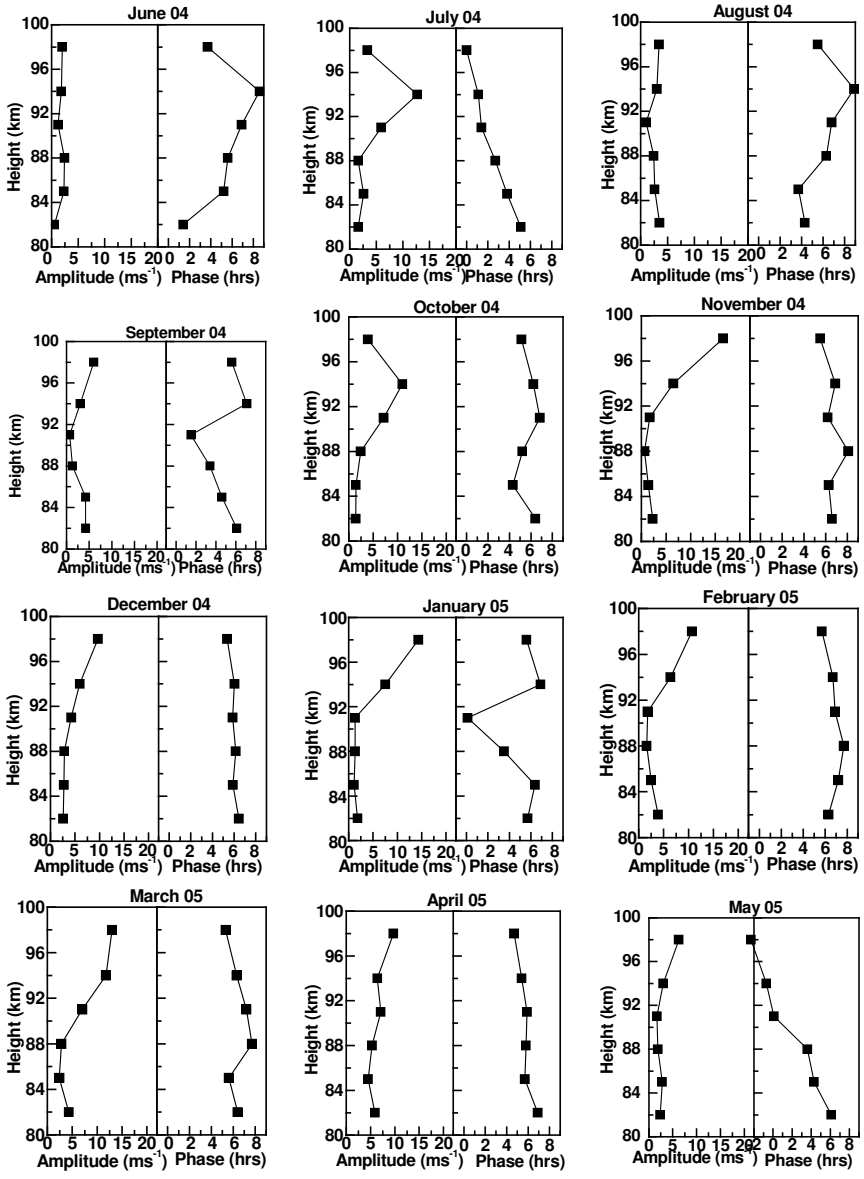

Fig. 8. Same as Fig. 3, but for meridional terdiurnal tides.

by Reddi and Ramkumar (1997) over Trivandrum. Using HRDI wind data, Smith (2000) observed terdiurnal tide with a maximum amplitude at 20° latitude.

The phase of the zonal wind remains constant at ∼8 h. The vertical wavelength is found to be very large. The phase remains constant at ∼6 h for meridional winds, during August, December, February and April as well, indicating a large vertical wavelength. During these months, zonal and meridional components are in almost quadrature polarization. During June and August, the phase of the meridional component increases with height up to 95 km. During July, September, January and May the phase decreases with height, and the vertical wavelength is very short, i.e. ∼16 km. The vertical wavelength is ∼50 km during October, November and March in the case of meridional winds. From the earlier observations from Trivandrum, Reddi and Ramkumar (1997) reported strong terdiurnal oscillations with a very large vertical wavelength (>100 km) and a smaller vertical wavelength of ∼20 km. Other observations of terdiurnal oscillations over tropical latitudes were reported by Bernald et al. (1981) over Puerto Rico (18° N), with a large vertical wavelength and sometimes as low as 50 km. Roper et al. (1993) also reported a significant amplitude of the terdiurnal oscillation over Arecibo.

Terdiurnal tides are produced by various physical processes, such as direct generation by solar thermal heating,

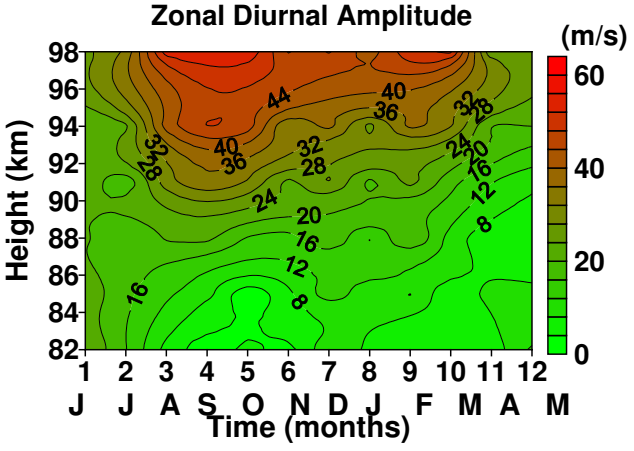

Fig. 9. Time-height contours of zonal diurnal amplitude showing the seasonal variation starting from June 2004 to May 2005. Contour intervals are 4 ms^{-1}.

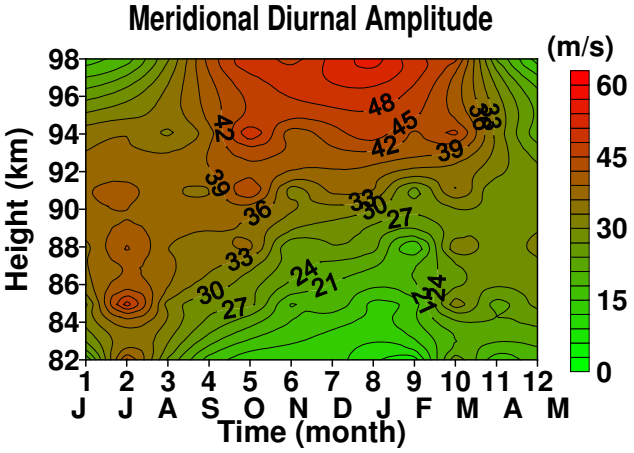

Fig. 10. Same as Fig. 9 but for meridional diurnal tide.

nonlinear interaction between the diurnal and semidiurnal tides, and tidal/gravity wave interaction. Based on both theoretical and observational studies Glass and Fellows (1975) and Teitelbaum et al. (1989) suggested that the terdiurnal tide could be produced by the nonlinear interaction between diurnal and semidiurnal tides. Miyahara and Forbes (1991) presented quantitative time dependent calculations, demonstrating that a diurnal tide can modulate the momentum deposition of gravity waves into the meanflow and hence produce a secondary oscillation near the 8-h and 12-h periods.

Classical or linear tidal oscillations are treated theoretically as first order perturbations, which are forced by solar heating. The solar driven or linear terdiurnal tides have large vertical wavelengths (Teitelbaum et al., 1989). Higher order effects are forced by combination of the primary wave field. The nonlinear mixing of diurnal and semidiurnal oscillations gives (Thayapparan, 1997)

$$u \propto \cos\left[2\pi\left(\frac{1}{T_{12}}+\frac{1}{T_{24}}\right)t - 2\pi\left(\frac{1}{\lambda_{12}}+\frac{1}{\lambda_{24}}\right)z + \Phi_1\right] + \cos\left[2\pi\left(\frac{1}{T_{12}}-\frac{1}{T_{24}}\right)t - 2\pi\left(\frac{1}{\lambda_{12}}-\frac{1}{\lambda_{24}}\right)z + \Phi_2\right], \quad (1)$$

where u is the zonal or meridional wind, T the period, λ the wavelength, Φ is the phase, t the time in hours. Among the forced waves, the one with the frequency and wavenumber equal to the sum of the frequencies and wavenumbers of the diurnal and semidiurnal tides is a terdiurnal tide. The other wave with the frequency and wavenumber equal to the difference of the frequencies and wavenumber of the diurnal and semidiurnal tides is a secondary diurnal tide. When a diurnal tide with vertical wavelength λ_1, nonlinearly interact with a semidiurnal tide of vertical wavelength λ_2, propagating in the same direction, a terdiurnal tide of vertical wavelength λ_z=$\lambda_1\lambda_2/(\lambda_1+\lambda_2)$ is produced (Reddi and Ramkumar, 1997). The observed vertical wavelength of the zonal and meridional diurnal tide in the present study is ∼25 km. The observed vertical wavelength of the meridional semidiurnal tide varies from ∼40 km to 64 km. The vertical wavelength calculated for the terdiurnal tide, using the above equation, varies from 15 km to 25 km and the observed vertical wavelength of the meridional terdiurnal tide varies from 15 km to 50 km. The calculated and observed vertical wavelength of the meridional terdiurnal tide is in good agreement during September and May. During all the other months the observed vertical wavelength is 2–3 times larger than the calculated value for the nonlinearly generated terdiurnal tide, except for January. This result thus shows an observational evidence of a possible nonlinear interaction between the diurnal and semidiurnal tides during some of the months. But the vertical wavelength of the zonal terdiurnal tide is observed to be very large during all the 12 months. This suggests other possibilities of terdiurnal tidal generation, such as direct solar heating, tidal/gravity wave interaction and changes in the excitation sources in the lower atmosphere.

3.4 Seasonal variation

Figure 9 shows the time-height section of the diurnal tidal amplitudes for zonal winds. The seasonal variation of tidal activity in the MLT region is clearly revealed from this figure. The tidal amplitudes show maximum activity above 90 km. The maximum value is observed during September, October, February and March, i.e. during the autumnal and vernal equinox. Earlier observations also showed that diurnal tides maximize over low latitudes and are strongest in the equinoxes (Burrage et al., 1995a, b; Mc Landress et al., 1996; Reddi and Ramkumar, 1997; Gurubaran and Rajaram, 1999). Figure 10 shows the seasonal variation of diurnal tidal amplitudes for meridional winds. In meridional wind as well, the maximum tidal activity is observed above 90 km. The enhanced activity is observed during December–January (winter). During June and July (summer), maximum meridional amplitudes are observed below 90 km. The diurnal tidal

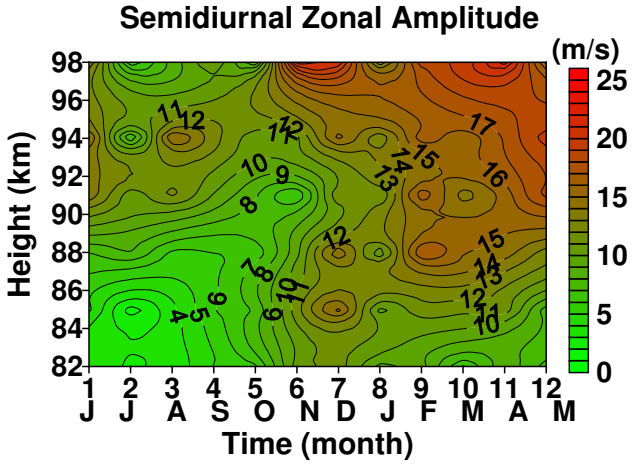

Fig. 11. Same as Fig. 9 but for zonal semidiurnal tide.

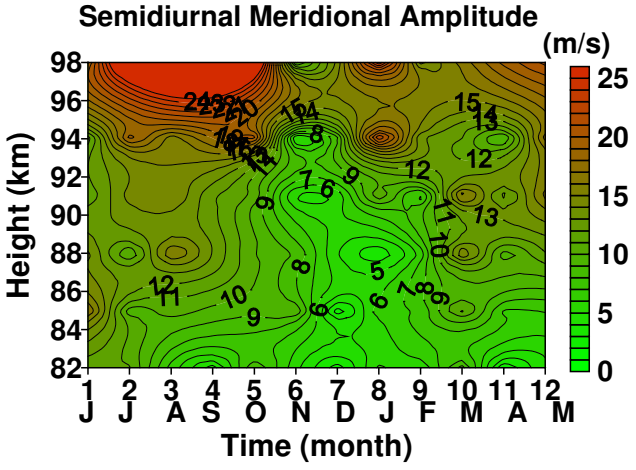

Fig. 12. Same as Fig. 9 but for meridional semidiurnal tide.

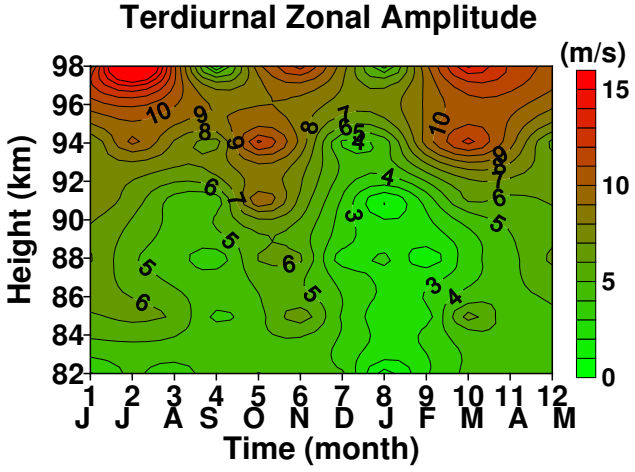

Fig. 13. Same as Fig. 9 but for zonal terdiurnal tide.

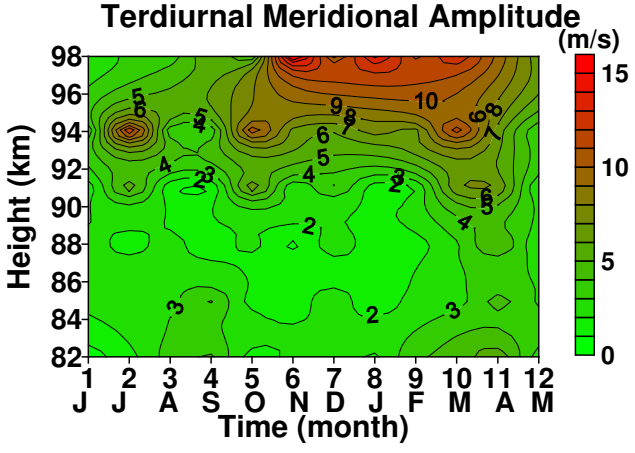

Fig. 14. Same as Fig. 9 but for merdional terdiurnal tide.

amplitudes show signatures of semiannual variability. Hagan et al. (1999) reported pronounced SAO in the meridional diurnal wind amplitude observed by HRDI over 20° latitude at 95-km altitude. They attributed this feature to seasonally varying gravity wave drag and eddy dissipation on the diurnal tide. They could reproduce the observed SAO in diurnal tides using the GSWM-98 model by including seasonally varying forcing, dissipation and meanflow effects. Seasonal variations of diurnal tides may be related to changes in the source strengths, such as the latent heat release associated with tropical deep convective activity (Forbes et al., 1997; Hagan et al., 1997), gravity wave variances in the upper stratosphere, which are expected to play an important role in modulating tidal amplitude (Wu and Jiang, 2005), or due to the nonlinear interaction between quasi-stationary planetary waves and the tidal oscillation (Oberheide et al., 2005).

Figures 11 and 12 show the seasonal variation of the amplitude of zonal and meridional semidiurnal tides. Maximum amplitudes are observed during December–March, i.e. winter and vernal equinox in the case of the zonal semidiurnal tide. The meridional semidiurnal tide shows maximum amplitudes during June to September. Burrage et al. (1995a, b), using HRDI wind data, and McLandress et al. (1996), with WINDII data, observed that the semidiurnal variability in the meridional wind in the equatorial region is maximum from April to August, which is consistent with the present results. They also observed that the variability in zonal semidiurnal component in the equatorial region is weak.

Seasonal variations of amplitude of zonal and meridional terdiurnal tide are shown in Figs. 13 and 14, respectively. Maximum zonal terdiurnal amplitudes are observed in July, October, March and April. Meridional terdiurnal amplitudes are larger during October, November, January, February and March. The variability of the meridional terdiurnal component is similar to the meridional diurnal component. This supports the hypothesis that the terdiurnal component could be generated by the nonlinear interaction between the diurnal and semidiurnal tide or by diurnal tidal/gravity wave interaction.

4 Summary and concluding remarks

This paper reports the results from SKiYMET radar observations at Trivandrum (8° N, 77° E) during June 2004–May 2005. The diurnal tidal component is observed to be prominent throughout the period of observation. The amplitude of the meridional diurnal tide is stronger than that of the zonal diurnal tide. The semidiurnal and terdiurnal tidal components are also found to be strong. The amplitude of the diurnal components attains a maximum of $\sim$50 ms^{-1}, and that of the semidiurnal and terdiurnal components are $\sim$20 ms^{-1} and 10 ms^{-1}, respectively. The phase structure of all three components shows a decreasing trend with altitude, indicating vertical propagation. The observed amplitudes and phases of the diurnal and semidiurnal tides are compared with the GSWM02 model. The observed amplitudes are equal to or greater than the model values. The observed and model phase structures are similar.

The vertical wavelength of the diurnal tidal components is found to be $\sim$25 km. The observed features of the diurnal components indicated the presence of the (1,1) mode. The vertical wavelength of the semidiurnal tide is found to be $>$100 km, which indicates that the (2,2) mode is prominently present. Sometimes higher order semidiurnal modes are also observed, as indicated by smaller vertical wavelengths (40–50 km) during some months. The vertical wavelength of the terdiurnal tide suggests that the observed terdiurnal tides are produced by various sources, such as direct solar heating, nonlinear interaction between diurnal and semidiurnal tides, and by tide/gravity wave interaction.

Prominent seasonal variation is observed in tidal characteristics. The diurnal tidal components are strong during two equinoxes. Semidiurnal zonal tides are stronger during the winter and vernal equinox, and meridional semidiurnal tides are strong during the summer and vernal equinox. Zonal terdiurnal amplitudes are stronger during equinoxes. Meridional terdiurnal amplitudes are strong during the winter and vernal equinox. Observed seasonal variation of various tidal modes can be attributed to the variation in the forcing and dissipation mechanisms. Detailed studies on these aspects will be pursued with a larger database.

This is the most powerful SKiYMET radar operational over the globe. The observations using this radar from the equatorial region will serve as an input to the global tidal studies under the program "CAWSES" (Climate And Weather of Sun Earth System).

Acknowledgements. The SKiYMET radar installed at Space Physics Laboratory was sanctioned under the 10th five year plan of Department of Space, India. The authors would like to acknowledge the support and encouragement provided by Chairman, ISRO, Director, VSSC and Director, SPL for installing the radar at our laboratory. The contributions from the team of engineers from Genesis Software Pty. Ltd, Australia and W. K. Hocking, Mardoc. Inc. Ltd., Canada, are well appreciated in successfully commissioning the radar facility. The authors are grateful to M. Hagan for the GSWM02 values of tidal oscillations taken from website. We acknowledge the services of M. Shajahan, M. Nair and Smt. L. Sarala for taking care of the system. The authors (V. Deepa and M. Antonita) are thankful to ISRO for providing Research fellowships.

Topical Editor U.-P. Hoppe thanks two referees for their help in evaluating this paper.

References

Avery, S. K., Vincent, R. A., Phillips, A., Manson, A. H., and Fraser, G. J.: High-latitude tidal behavior in the mesosphere and lower thermosphere, J. Atmos. Terr. Phys., 51, 595–608, 1989.

Bernard, R., Fellous, J. L., Massebeuf, M., and Glass, M.: Simultaneous meteor radar observations at Monpazier (France, 44° N), and Punta Borinquen (Puerto-Rico, 18° N), I, Latitudinal variations of atmospheric tides, J. Atmos. Terr. Phys., 43, 525–533, 1981.

Burrage M. D., Wu, D. L., Skinner, W. R., Ortland, D. A., and Hays, P. B.: Latitude and seasonal dependence of the semidiurnal tide observed by the high-resolution Doppler imager, J. Geophys. Res., 100, 11 31–11 321, 1995a.

Burrage M. D., Hagan, M. E., Skinner, W. R., Wu, D. L., and Hays, P. B.: Long-term variability in the solar diurnal tide observed by HRDI and simulated by the GSWM, Geophys. Res. Lett., 22, 2641–2644, 1995b.

Chang, J. L. and Avery, S. K.: Observations of the diurnal tide in the mesosphere and lower thermosphere over Christmas Island, J. Geophys. Res., 102, 1895–1907, 1997.

Countryman, I. D. and Dolas, P. M.: Observations on tides in the equatorial mesosphere, J. Geophys. Res., 87, 1336–1342, 1982.

Forbes, J. M.: Atmospheric Tides 1, Model description and results for the solar diurnal component, J. Geophys. Res., 87, 5222–5240, 1982.

Forbes, J. M. and Groves, G. V.: Diurnal propagating tides in the low-latitude middle atmosphere, J. Atmos. Terr. Phys., 49, 153–164, 1987.

Forbes, J. M. and Vial, F.: Monthly simulation of the solar semidiurnal tide in the mesosphere and lower thermosphere, J. Atmos. Terr. Phys., 51, 649–661, 1989.

Forbes, J. M., Hagan, M. E., Zhang, X., and Hamilton, K.: Upper atmosphere tidal oscillations due to latent heat release in the tropical troposphere, Ann. Geophys., 15, 1165–1175, 1997, http://www.ann-geophys.net/15/1165/1997/.

Fraser, G. J., Portnyagin, Y. I., Forbes, J. M., Vincent, R. A., Lysenko, I. A., and Makarov, N. A.: Diurnal tide in the Antarctic and Arctic mesosphere/lower thermosphere region, J. Atmos. Terr. Phys., 57, 383–393, 1995.

Glass, M. and Fellous, J. L.: The eight-hourly (terdiurnal) component of atmospheric tides, Space Res., XV, 191–197, 1975.

Gurubaran, S. and Rajaram, R.: Long-term variability in the mesospheric tidal winds observed by MF radar over Tirunelveli (8.7° N, 77.8° E), Geophys. Res. Lett., 26, 1113–1116, 1999.

Hagan, M. E., Forbes, J. M., and Vial, F.: On modeling migrating solar tides, Geophys. Res. Lett., 22, 893–896, 1995.

Hagan, M. E.: Comparative effects of migrating solar sources on tidal signatures in the middle and upper atmosphere, J. Geophys. Res., 101, 21 213–21 222, 1996.

Hagan, M. E., Mc Landress, C., and Forbes, J. M.: Diurnal tidal variability in the upper mesosphere and lower thermosphere,

Ann. Geophys., 15, 1176–1186, 1997, http://www.ann-geophys.net/15/1176/1997/.

Hagan, M. E., Burrage, M. D., Forbes, J. M., Hackney, J., Randel, W. J., and Zhang, X.: GSWM-98: Results for migrating solar tides, J. Geophys. Res., 104, 6813–6828, 1999.

Hagan, M. E. and Roble, R. G.: Modeling diurnal tidal variability with the National Center for Atmospheric Research thermosphere-ionosphere-mesosphere-electrodynamics general circulation model, J. Geophys. Res., 106, 24 869–24 882, 2001.

Hagan, M. E. and Forbes, J. M.: Migrating diurnal tides in the upper atmosphere excited by tropospheric latent heat release, J. Geophys. Res., 107, doi:10.1029/2001JD001236, 2002.

Hagan, M. E. and Forbes, J. M.: Migrating semidiurnal tides in the upper atmosphere excited by tropospheric latent heat release, J. Geophys. Res., 108, doi:10.1029/2002JA009466, 2003.

Harper, R. M.: Some results on mean tidal structure and day-to-day variability over Arecibo, J. Atmos. Terr. Phys., 43, 255–262, 1981.

Hocking, W. K., Fuller, B., and Vandepeer, B.: Real time determination of meteor-related parameters utilizing modern digital technology, J. Atmos. Sol. Terr. Phys., 63, 155–169, 2001.

Manson, A. H., Meek, C. E., Avery, S. K., and Tetenbaum, D.: Comparison of mean wind and tidal fields at Saskatoon (52° N, 107° W) and Poker Flat (65° N, 147° W) during 1983/1984, Phys. Scr., 37, 169–177, 1988.

Manson, A. H., Meek, C. E., Hagan, M. E., Hall, C., Hocking, W., MacDougall, J., Franke, S. J., Riggin, D., Fritts, D. C., Vincent, R. A., and Burrage, M. D.: Seasonal variations of the semidiurnal and diurnal in the MLT: multi-year MF radar observations from 2–70° N and the GSWM tidal model, J. Atmo, Sol. Terr. Phys., 61, 809–828,1999.

Manson, A. H., Meek, C. E., Hagan, M. E., et al.: Seasonal variations of the semidiurnal and diurnal tides in the MLT: Multi-Year MF Radar observations from 2–70° N, Modelled Tides (GSWM, CMAM), Ann. Geophys., 20, 661–677, 2002a.

Manson, A. H., Luo, Y., and Meek, C.: Global distributions of diurnal and semi-diurnal tides: observations from HRDI-UARS of the MLT region, Ann. Geophys., 20, 1877–1890, 2002b.

Mathews, J. D.: Measurements of the diurnal tides in the 80–100 km altitude range at Arecibo, J. Geophys. Res., 81, 4671–4677, 1976.

Mc Landress, C., Shepherd, G. G., and Solheim, B. H.: Satellite observations of thermospheric tides: Results from the Wind Imaging Interferometer on UARS, J. Geophys. Res., 101, 4093–4114, 1996.

Miyahara, S. and Forbes, J. M.: Interaction between gravity waves and the diurnal tide in the mesosphere and lower thermosphere, J. Meteorol. Soc. Japan, 69, 523–532, 1991.

Morton, Y. T., Lieberman, R. S., Hays, P. B., Ortland, D. A., Marshall, A. R., Wu, D., Skinner, W. R., Burrage, M. D., Gell, D. A., and Yee, J. -H.: Global mesospheric tidal winds observed by HRDI on board UARS, Geophys. Res. Lett., 20, 1262–1266,1993.

Oberheide, J., Wu, Q., Ortland, D. A., Killeen, T. L., Hagan, M. E., Roble, R. G., Niciejewski, R. J., and Skinner, W. R.: Nonmigrating tides as measured by the TIMED Doppler interferometer: Preliminary results, Adv. Space. Res., 35, 1911–1917, 2005.

Pancheva, D., Mitchell, N. J., Hagan, M. E., et al.: Global scale tidal structure in the mesosphere and lower thermosphere during the PSMOS campaign of June-August 1999 and comparisons with the global-scale wave model, J. Atmos. Sol. Terr. Phys., 64, 1011–1035, 2002.

Portnyagin, Y. I., Forbes, J. M., Fraser, G. J., Vincent, R. A., Lysendo, I. A., and Makarov, N. M.: Dynamics of the Antarctic and Arctic mesosphere/lower thermosphere regions, Adv. Space Res., 12, 89–96, 1992.

Reddi, C. R., Rajeev, K., and Geetha, R.: Tidal winds in the radio-meteor region over Trivandrum (8.5° N, 77° E), J. Atmos. Terr. Phys., 55, 1219–1231, 1993.

Reddi, C. R. and Ramkumar, G.: Climatologies of tidal winds in the radio-meteor region over Trivandrum (8° N), J. Atmos. Sol. Terr. Phys., 59, 1757–1777, 1997.

Roper, R., Adams, G. W., and Brosnahan, J. W.: Tidal winds at mesopause altitudes over Arecibo (10° N, 67° W), 5-11 April 1989 (AIDA '89), J. Atmos. Terr. Phys., 55, 289–312, 1993.

Smith, A. K.: Structure of the terdiurnal tide at 95 km, Geophys. Res. Lett., 27, 177–180, 2000.

Talaat, E. R. and Lieberman, R. S.: Nonmigrating diurnal tides in Mesospheric and Lower-Thermospheric winds and temperatures, J. Atmos. Sci., 56, 4073–4087, 1999.

Teitelbaum, H., Vial, F., Mansion, A. H., Giraldez, R., and Massebeuf, M.: Nonlinear interacation between the diurnal and terdiurnal tides: diurnal and diurnal secondary waves, J. Atmos. Terr. Phys., 51, 627–634, 1989.

Tetenbaum, D., Avery, S. K., and Riddle, A. C.: Observations of mean winds and tides in the upper mesosphere during 1980-1984, using the Poker Flat, Alaska, MST radar as a meteor radar, J. Geophys. Res., 91, 14 539–14 555, 1986.

Thayapparan, T.: The terdiurnal tide in the mesosphere and lower thermosphere over London, Canada (43° N, 81° W), J. Geophys. Res., 102, 21 695–21 708, 1997.

Tsuda, T., Ohnishi, K., Isoda, F., et al.: Coordinated radar observations of atmospheric diurnal tides in equatorial regions, Earth Planets Space, 51, 579–592, 1999.

Wu, D. L. and Jiang, H.: Interannual and seasonal variations of diurnal tide, gravity wave, ozone, and water vapor as observed by MLS during 1991–1994, Adv. Space. Res., 35, 1999–2004, 2005.

Zhang, S. P., Thayer, J. P., Roble, R. G., Salah, J. E., Shepherd, G. G., Goncharenko, L. P., and Zhou, Q. H.: Latitudinal variations of neutral wind structures in the lower thermosphere for the March equinox period, J. Atmos. Sol. Terr. Phys., 66, 105–117, 2004.